ACDIV-2015-01
May, 2015

REVISION OF THE IMPEDANCE MODEL FOR THE INTERPRETATION OF THE SINGLE BUNCH MEASUREMENTS AT ALBA

T.F. Günzel and U.Iriso
ALBA Synchrotron, Cerdanyola del Vallès, Barcelona, Spain

Abstract

Recently [1] we were able to explain 65% of the measured vertical single bunch detuning with the developed transverse impedance model. In this note we show the improvements of the impedance model we could achieve in the meantime. We included a better bunch length parametrisation of all contributions. Moreover, the geometrical impedance of several vacuum chamber elements was recalculated with GdfidL [2] and the impedance of a couple of elements neglected so far was included in the budget. ImpedanceWake2D [3] was used for the computation of the (resistive) wall impedance.

Accelerator Division
Alba Synchrotron Light Source
Ctra. BP 1413 Km. 3,3
08290 Cerdanyola del Valles, Spain

REVISION OF THE IMPEDANCE MODEL FOR THE INTERPRETATION OF THE SINGLE BUNCH MEASUREMENTS AT ALBA

T.F. Günzel and U.Iriso, ALBA Synchrotron, Cerdanyola de Vallés, Spain

Abstract

Recently [1] we were able to explain 65% of the measured vertical single bunch detuning with the developed transverse impedance model. In this note we show the improvements of the impedance model we could achieve in the meantime. We included a better bunch length parametrisation of all contributions. Moreover, the geometrical impedance of several vacuum chamber elements was recalculated with GdfidL [2] and the impedance of a couple of elements neglected so far was included in the budget. ImpedanceWake2D [3] was used for the computation of the (resistive) wall impedance.

INTRODUCTION

In the past at different accelerators significant differences between the computed and measured single bunch detuning were observed [4, 5]. However, the work [6] shows that achieving an agreement is not impossible. An accurate computation of the impedance gains importance as the construction of ultralow emittance sources pushes the instability thresholds to limits which are hardly feasible. This note describes the work carried out to carefully benchmark impedance measurements with the computated impedance at the ALBA storage ring. On one side, measurements were taken varying different machine parameters like the RF-voltage and the gap of the in-vacuum undulators. On the other hand, careful simulations using GdfidL and ImpedanceWake2D(IW2D) were carried out using an experimental bunch parametrisation.

IMPROVEMENT OF THE IMPEDANCE MODEL

The key point of this work consists in the upgrade of the underlaying vertical impedance model. The model contains two parts, the impedance of geometrical origin – also called broadband impedance – and impedance related to the resistivity of the vacuum chamber walls and that part of space charge that only depends on the chamber extension – the wall impedance. The broadband impedance (BBI) is computed by simulation of electromagnetic wake fields in corresponding vacuum chambers with the program GdfidL [2] whereas the wall impedance is computed analytically. For this work the wall impedance was computed for the first time with ImpedanceWake2D.

Wall Impedance

IW2D allows to calculate the wall impedance for a round or fully flat beam pipe consisting of n different material layers of constant thickness. Table 1 shows the list of chambers analyzed by IW2D. The code solves the Maxwell equations exactly and should be therefore best adapted to the problem (this is only partly true as no chamber wall is an assembly of layers of exactly constant thickness).

Comparing the impedance spectra of IW2D with those of the RW-models of the precedent work [1] rather good agreement was found even for multi-layer chamber walls. Actually, IW2D computes in the range $f \in [5, 50]$GHz an imaginary part slightly smaller than the one given by the traditional RW-formula for mono-layers (Fig. 1) as well as for most multi-layer chamber walls.[1] The real part was slightly higher though.

Table 1: Vacuum Chambers Analyzed by IW2D

Chamber type	**Assumed Layers**
In-vac undulator(open/closed)	Cu/Ni/CoSm
NEG-coated Al-chamber	NEG/Al/Air
Ti-coated ceramic chamber	Ti/Al_2O_3/Air/Ferrit
Wiggler chamber	Cu/Air
Cavities	Cu/Air
Different SS[2]-chambers	SS/Air

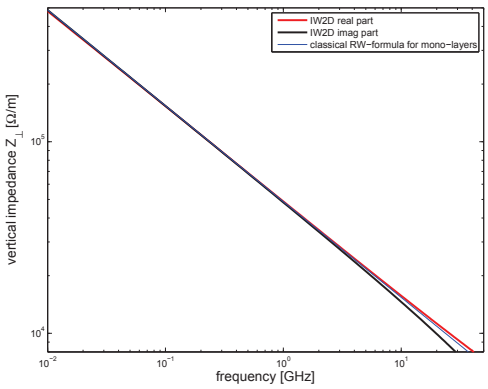

Figure 1: wall impedance of std vacuum chamber. At high frequency the imaginary part is smaller than both the real part and the one given by the classical RW-formula for mono-layers.

Geometrical Impedance

For the improvement of the geometrical impedance a revision of the geometrical models of the taper-dominated geometries and their annexes (table 2) was done. Furthermore, element geometries were equipped with the missing pump grids and their wake-fields simulated. They are all finally decomposed in monopolar, dipolar and quadrupolar

[1] formulas based on the work of [7]

[2] SS: stainless steel

part the two latter of which are kept. Finally, quantity, position and vertical β-function of most elements included in the impedance budget were revisioned. Several deviations from the real vacuum chamber assembly were found, their correction increased vert. impedance by a sensible amount. Flanges at only at 8mm-gap chambers were discovered to be of 150mm diameter, larger than the usual Spigot flanges of 100mm diameter which account for the impedance increase to a large extent. Above all β-weighted vert. impedance could be gained from most of the taper-dominated geometries, in particular from the invacuum undulator geometry. Figure 2 shows the imaginary part of the dipolar β-function weighted geometrical impedance obtained by fourier transform from the wake field.

Table 2: GdfidL-simulated vacuum chambers with their resulting dipolar broadband impedance. The porcentual gain in each element impedance due to the revision is included.

Chamber	Z_V [kΩ/m]
Horizontal scraper& pump mesh	0.24(+99.999%)
Cavity pipe & tapers	1.13(+20%)
Wiggler chamber & tapers	6.08(+9.5%)
Low-gap Al chamber & tapers	8.21(+20.3%)
In-vacuum undulators	21.75(+34.6%)
Pinger chamber(NEW)	0.64(+100%)

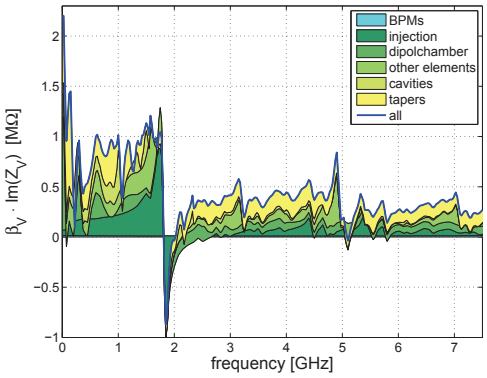

Figure 2: Imaginary part of the BBI of various ALBA elements and the total BBI.

COMPARISON WITH THE MEASUREMENTS

Computation of the Detuning Slopes

In this study it is intended to avoid most of the parametrisations which were used in the precedent study [1] in order not to distort the data. Therefore instead of using an Vlasov-eq. solver for the theoretical calculation of the detuning and mode coupling the impedance spectra $Z_\perp(\omega)$ just are weighted with the corresponding bunch spectrum of each measured bunch current I and integrated over angular frequency ω to obtain kick factors $\kappa_\perp$:

$$\kappa_\perp = \frac{1}{\pi}\int_0^\infty Im(Z_\perp(\omega))\exp(-(\sigma_\tau\omega)^2)d\omega \qquad (1)$$

For the accurate computation of the kick factors the correct bunch lengthes are required which stem from bunch length parametrisations with current based on the bunch length measurements. For each different RF-voltage a different bunch length parametrisation was generated. Finally, the betatron detuning $\Delta\nu_\beta$ can be easily obtained from the kick factors by the simple relation which does not contain the bunch length σ_τ explicitly:

$$\Delta\nu_\beta(I) = \frac{I}{2\omega_0(E/e)}\sum(\beta\kappa)_\perp(\sigma_\tau(I)) \qquad (2)$$

E/e stands for the elementary charge normalized beam energy and ω_0 for the angular revolution frequency. Table 3 shows a breakdown of β-weighted kick factors for the ALBA storage ring.

The obtained detuning can be directly compared with the measured detuning. A additional normalisation on the (zero current) synchrotron tune ν_{s0} can be applied, but is only necessary if data sets taken at different RF-voltages are compared. This approach resigns the comparison of the theoretical and the measured TMC-instability threshold. However, to show to which extent the agreement of single bunch detuning is reached it is not necessary.

Table 3: Computed Vertical Impedance Budget @σ_τ = 22ps

Type	**Geometrical** [$\frac{kV}{pC}$]	**RW** [$\frac{kV}{pC}$]
Dipolar $(\beta\kappa)_V$	5.92	7.66
Quadrupolar$(\beta\kappa)_V$	1.83	3.90
Total $(\beta\kappa)_V$ = 19.31	7.75	11.56
Total $(\beta Z_{\mathrm{eff}})_V = 1504k\Omega$		

Measurements and Results

The measurements of the vertical single bunch detuning at $\xi = 0$ were repeated at different RF-voltages 1.4MV, 1.56MV, 1.83MV, 2.1MV and 2.3MV and other settings. Furthermore after the installation of a pinger chamber, the measurements were repeated in order to observe the pinger's impact on the tranverse impedance [8]. Finally, different data sets were taken at closed and open invacuum undulators (2 undulators). The most recent data sets were taken even during injection using shot-to-shot tune measurements. This technique provides more accurate vertical tune values and reduces significantly the experiment duration. Each data set included bunch length measurements at different bunch intensities.

The computed detuning slopes well follow the measured slopes upon variation of the RF-voltage (Fig. 3). The detuning slopes are computationally reproduced up to 75% (Fig. 4) which is quite satisfactory. The computed slopes depend sensibly on the bunch length parametrisation and should for

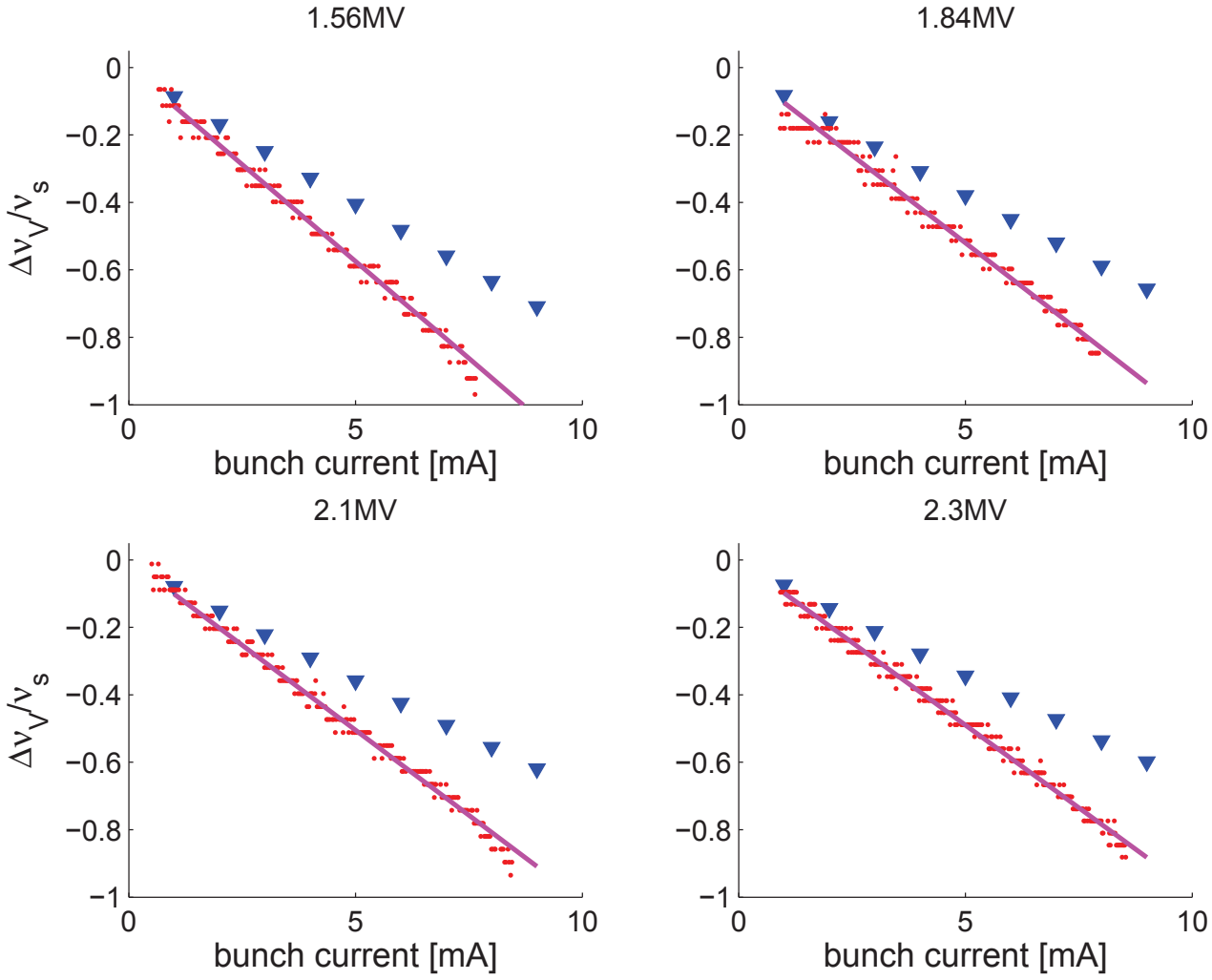

Figure 3: Comparison of measured and computed single bunch detuning at $\xi = 0$ for different RF-voltages, measured detuning (red), fitted detuning (magenta) and computed detuning (blue).

quantitative evaluation be backed up with threshold measurements. In particular, due to an improved simulation of the tapers of the in-vacuum undulators their model now reproduces 62% of the β-function weighted effective impedance $(\beta Z_V) = 256k\Omega$ compared to the 44% from the previous work [1]. Nevertheless the discrepancy between measurement and impedance model seems to be most pronounced for complex structured chambers.

CONCLUSION

An improvement of the computed impedance budget could be achieved by the addition of up to now overlooked vacuum elements and a more detailed taper simulation of the low-gap chambers, in particular the in-vacuum undulators in the ALBA-ring. IW2D, however, provided impedance values which were even slightly smaller than those of the precedent work [1], this reduction of impedance could be overcompensated by an even larger gain of geometrical impedance. One could attribute the missing 25% vertical impedance to the injection kickers as their geometry is similar to the pinger geometry. However, as long as the large measured pinger impedance exceeding substantially the expectation is not backed up by computation [8] this is a preliminary conclusion and the investigations have to pursue, especially regarding the influence of the bunch length parametrisation.

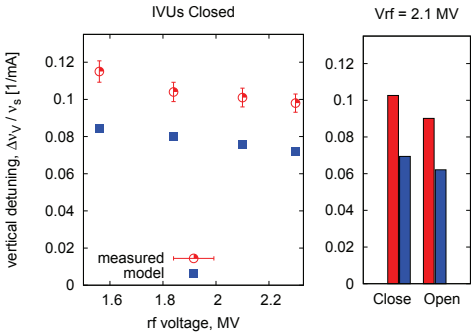

Figure 4: Vertical detuning under different conditions.

REFERENCES

[1] T.F.Günzel et al., "Analysis of single bunch measurements at the ALBA storage ring", TUPRI052, IPAC 2014, p.1686.

[2] W.Bruns, GdfidL, www.gdfidl.de

[3] N. Mounet http://impedance.web.cern.ch/impedance/Codes/ImpedanceWake2D/user_manual_todate.txt

[4] T.F.Günzel. "The transverse coupling impedance of the storage ring at the ESRF ", Phys.Rev.-STAB 9, 114402.

[5] R.Nagaoka et al. "Beam instability Observations and analysis at Soleil", PAC'07, Albuquerque, WEOBC01, p.2019.

[6] H.Bartosik et al. "TMCI thresholds for LHC single bunch in the CERN SPS and comparison with simulations", IPAC'14, Dresden, Germany, p.1407.

[7] A. Burov and V. Lebedev, "Transverse Resistive wall impedance for multi-layer flat chambers", EPAC'02, Paris, p.1455.

[8] T.F.Günzel et al., "Beam-based Impedance characterization of the ALBA pinger magnet", *These Proceedings*, IPAC'15, Richmond VA, USA (2015).